Microscopic Dynamics and Macroscopic Mechanical Deformation of Poly(*p*-phenyleneterephthalamide) Fibers‡

D. J. Schaefer, R. J. Schadt,† K. H. Gardner, V. Gabara, S. R. Allen, and A. D. English*

DuPont Central Research and Development and DuPont Advanced Fibers Systems, Experimental Station, Wilmington, Delaware 19880-0356

Received August 26, 1994; Revised Manuscript Received November 28, 1994®

ABSTRACT: Deuterium NMR methods are used to characterize the dynamic structure of PPTA [poly(*p*-phenyleneterephthalamide)] fiber as a function of tension. Spin−lattice relaxation results indicate that the high-frequency component of the dynamic structure is not significantly altered by the fiber-spinning process or by the application of tensile stress to the fiber and as such does not differ from that of the as-polymerized polymer. Quadrupolar-echo line shapes reflect the high degree of order as well as the motional heterogeneity of the fiber bundle. The application of a tensile stress equivalent to 55% of the breaking strength of the fiber bundle alters the ^{2}H NMR line shape, thus reflecting the coupling of macroscopic stress and microscopic dynamic structure through the enhancement of the phenylene ring dynamics. Two-dimensional ^{2}H NMR methods are used to characterize the chain axis orientational distribution of a continuous fiber bundle. Simulations of the experimental spectra are consistent with a Gaussian distribution of orientations with a standard deviation of no larger than 5°; this result is in good agreement with previous X-ray results and differs substantially from previous solid-state NMR approaches which utilized *chopped* fibers.

Introduction

Poly(*p*-phenyleneterephthalamide), PPTA, can be spun into fibers that exhibit high tenacity, modulus, and thermal stability. The outstanding mechanical properties of these fibers are largely attributable to the high degree of order and orientation that they possess. The degree of order in fibers, films, and as-polymerized polymer is controlled to a large extent by the process utilized when the polymer is precipitated from solution. The relationship of the microscopic order and dynamic structure to the macroscopic mechanical properties has been of interest for many years. This paper deals with three major themes: first, the effect that the fiber spinning process and subsequent posttreatment has on the dynamic structure of the PPTA fiber; second, the influence of the application of macroscopic tensile stress to the fiber on the microscopic dynamic structure; third, the chain axis orientational distribution determined by a variety of multidimensional NMR methods and comparison of these results to classical X-ray analysis.

In previous papers, the segmental dynamics of the terephthalamide rings,[1−3] *p*-phenylenediamine rings,[4] and amide sites[5,6] of PPTA have been characterized over a wide temperature range with ^{2}H NMR methods. These studies characterized the dynamic structure[7] of PPTA in terms of sites associated either with the surfaces of crystallites or the interior of the crystallites. The dynamic structure of the polymer differs substantially at the three chemically distinct sites (amide, terephthalamide rings, and diamine rings) and is seen to be extremely heterogeneous on both the segmental and crystallite length scales.

The key to understanding the dynamic structure of PPTA polymer is provided by the ^{2}H NMR line shapes for the amide sites[5,6] which may be decomposed into a major component (~75%) associated with relatively rigid amide sites and a minor component (~25%) associated with mobile amide bonds (which execute large-angle reorientations). This behavior of the amide sites was determined to be essentially temperature independent over the range −184 to +228 °C. X-ray diffraction[6] shows that the crystallite size in the lateral dimension for the as-polymerized polymer is rather small (~35 Å), and this small size requires that a large fraction (~40%) of all amide sites must reside on a crystallite surface and hence ~20% of all amide sites in the entire crystal are not capable of forming a hydrogen bond. The differentiation of amide mobility is therefore identified as deriving from incompletely hydrogen-bonded sites located at the crystallite surface or defect regions of the highly crystalline polymer.[8] Additional evidence for the presence of two dynamically differentiated populations of amide groups in PPTA polymer is available from the ^{2}H NMR spin−lattice relaxation data where, over the temperature range −184 to +75 °C, the fractional population falls in the range 75 ± 10%; at higher temperatures (228 °C) this population is reduced to ~50% by the presence of considerable motion in nearby terephthalamide[3] and diamine rings.[4] [Additionally, the longer spin−lattice relaxation time component of the terephthalamide and diamine rings shows a virtually temperature independent population (near 75%) over the same temperature range.[4]] Thus it appears that it is the mobile amide sites which give rise to the spin−lattice relaxation time differentiation of not only the amide sites but also the terephthalamide and diamine ring sites over the temperature range −184 to +75 °C in PPTA polymer.

Examination of the ^{2}H NMR line shape data for the terephthalamide[1−3] and *p*-phenylenediamine[4] rings revealed that the *p*-phenylenediamine ring dynamic structure is characterized by a broad distribution of correlation times and that an even broader (or bimodal) distribution of correlation times characterizes the dynamics of the terephthalamide rings. These observations indicate that in addition to the fairly simple dynamic structure described above (crystallite surface

* To whom correspondence should be addressed.
† Current address: Hoffman-La Roche, Inc., 340 Kingsland St., Nutley, NJ 07110.
‡ Contribution No. 6965.
® Abstract published in *Advance ACS Abstracts,* January 15, 1995.

0024-9297/95/2228-1152$09.00/0

vs crystallite interior), each population must contain a variety of dynamical environments which reflect the heterogeneity of the dynamic structure within each population. It appears that the heterogeneity of the dynamic structure reflects not only the small dimensions of the crystallites perpendicular to the chain axis but also the concomitant proximity of all chains to a crystallite surface and hence a substantial probability of structural imperfections throughout the crystallite.

The structural response of aramid fibers to deformation has been investigated in a number of studies employing a variety of methods such as mechanical testing,[9-12] WAXS,[13,14] and Raman spectroscopy.[12,15-21] Initial investigations of structural changes associated with deformation of aramids emphasized a description focusing on a length scale of a few Ångstroms, specifically, the combination of bond stretching and bond angle deformation and better alignment and increased perfection of the crystallites.[9,10,22] Later descriptions focused on the supramolecular organization of aramid fibers, notably the pleated sheet structure[23] and its relationship to deformation.[24] Light scattering[25] results have shown that the stress dependence of the modulus corresponds to a progressive opening of the pleats,[26,27] which may be reversed upon unloading. Thus the response to deformation in aramid fibers can be attributed to structural changes that occur on length scales of ~1 to ~1000 Å. For polymers other than PPTA, solid-state NMR studies have found that molecular mobility is sensitive to mechanical deformation and that the results of these studies can be used to more extensively characterize the molecular motion and structure.[28-30] For example, the effect of tensile stress on the phenylene flips in polycarbonate has been recently studied by means of one- and two-dimensional ^{2}H NMR.[31-33]

Experimental Procedures

Material Synthesis. PPTA polymer, with selectively deuterated terephthalamide rings [PPTA-T(d_4)], was prepared by copolymerizing *p*-phenylenediamine with 99+% isotopically pure terephthaloyl-d_4 chloride in an 8% solution of $CaCl_2$ in *N*-methylpyrrolidone followed by precipitation in water.[34] The resulting as-polymerized polymer had an inherent viscosity of 6.6 dL/g (as measured as a 0.5 wt % solution in 100% sulfuric acid).

PPTA-T(d_4) fiber was air gap spun from a ~20% solution of PPTA-T(d_4) polymer in 100% H_2SO_4 at 80 °C through a 10-hole 3-mil-diameter spinneret (aspect ratio of 3) with an air gap of 0.5 cm, a solution jet velocity of 20 m/min, and a spin stretch factor of 6 into a 35-cm-long, 3 °C cold water bath. An inherent viscosity of 5.9 dL/g was measured for polymer isolated from the spin dope, indicating that no significant degradation of the polymer had taken place in the spinning solution.

The tensile properties of the fiber were determined after 24 h of conditioning of the fibers at 65% relative humidity and 70 °F (ASTM D1776) from 10-in. yarn breaks with an Instron 1122 frame equipped with a 50-lb load cell by following ASTM procedure D2256 and D885 with a twist-multiplier of 1.1 (ASTM D1423); the denier (d) was measured according to ASTM D1059 and MATM 7020.03. The values obtained were 24 g/d (3.1 GPa) tenacity, 3.7% ultimate elongation, and 550 g/d (70 GPa) modulus. Subsequent heat treatment of the never-dried 60-filament fiber (obtained by plying together six 10-filament bobbins of as-spun fiber) by passing it through a 1-ft oven at 275 °C at a rate of 10 ft/min under a tension of about 2 g/d produced a fiber with modified physical properties: 22 g/d (2.8 GPa) tenacity, 2.4% ultimate elongation, and 890 g/d (114 GPa) modulus. These sets of physical properties may be compared to those reported[35] for Kevlar 29 [23 g/d tenacity (3 GPa), 3.6% ultimate elongation, 480 g/d (62 GPa) modulus)] and Kevlar 49 [(23 g/d (3 GPa) tenacity, 2.5% ultimate elongation, 910 g/d (117 GPa) modulus].

The NMR sample consisted of the heat-treated PPTA-T(d_4) *continuous* fiber with an approximate denier of 130, wound in a loop with the two ends knotted together; the bundle had a denier of approximately 40 000 and a length of about 34 in. The tensile properties for bundles of the above dimension were found to be 15 g/d tenacity, 1.6% ultimate elongation, and 950 g/d modulus. This may be compared to the values found for a bundle assembled from Kevlar 49: 15 g/d tenacity, 1.6% ultimate elongation, and 990 g/d modulus.

X-ray Diffraction Measurements. X-ray diffractometry scans were collected in the symmetrical reflection mode using an automated Philips diffractometer (curved crystal monochromator, 1° divergence and receiving slits, and Cu Kα radiation). Samples were prepared for X-ray diffraction experiments by wrapping the fiber to make a ~1-mm-thick parallel array. Data were collected in a fixed time mode with a step size of 0.05° from 6 to 36° (2θ) at room temperature. Values for the apparent crystallite size, as determined from the (110) and the (200) reflections, were obtained for both the as-spun and heat-treated PPTA-T(d_4) fibers and are comparable to values reported for Kevlar 29 and Kevlar 49 fibers.[6]

X-ray diffraction patterns were also recorded for the fiber used in the NMR experiment with a vacuum flat plate camera (Ni-filtered Cu Kα) with a sample-to-film distance of 5 cm. The diffraction patterns were digitized, and order parameters, using the (200) reflections, for the as-spun and heat-treated PPTA-T(d_4) fibers were calculated. These order parameters did not show any significant deviation from values found for commercial Kevlar 29 and Kevlar 49 fibers.

NMR Measurements. ^{2}H NMR experiments were performed at room temperature with a Bruker MSL 200 NMR spectrometer operating at a resonance frequency of 30.72 MHz and utilizing a probehead (Doty Scientific, Inc.)[36] with a 5-mm saddle coil and a 90° pulse length of 4 μs. The probehead allows free passage of a vertically suspended *continuous* fiber bundle through the entire probe body. Tension on the fiber bundle was applied through the use of 31 steel plates with a total weight of ~300 kg, which was sufficient to elongate the fiber bundle by approximately 0.8%. [Control experiments indicated that over a period of 4 weeks this elongation increases to about 1% due to creep of the fiber.] The continuous fiber bundle is, to an extremely good approximation, aligned parallel to the external magnetic field, and no misalignment of individual fibers is assumed in any of the analyses. Fully and partially-relaxed ^{2}H NMR spectra were acquired using a quadrupolar-echo pulse sequence with delay times (τ) of 40, 80, and 160 μs between 90° pulses; additionally, spin–lattice relaxation times were measured via the saturation recovery method. 2D experiments were performed with a four- or five-pulse sequence which are described in detail elsewhere.[37,38]

Results and Discussion

Zero Stress. A previous comparison of ^{2}H NMR powder line shapes of PPTA-T(d_4) in both as-polymerized and chopped fiber forms indicated that the line shapes were not sensitive to the type of fiber formation process used in that study.[3] Furthermore, the spin–lattice relaxation values obtained for the chopped fiber sample were essentially identical within experimental error to that found for the as-polymerized polymer. Hence, the previously utilized process of fiber formation for PPTA-T(d_4) played no significant role in modifying the dynamics of the terephthalamide rings. The observed insensitivity of the NMR results to the type of fiber formation process previously used is now understood to be due to the fraction of sites located on the crystallite surfaces being similar for the as-polymerized polymer and the fiber.

Figure 1 shows quadrupolar echo line shapes of the PPTA-T(d_4) continuous fiber bundle at room tempera-

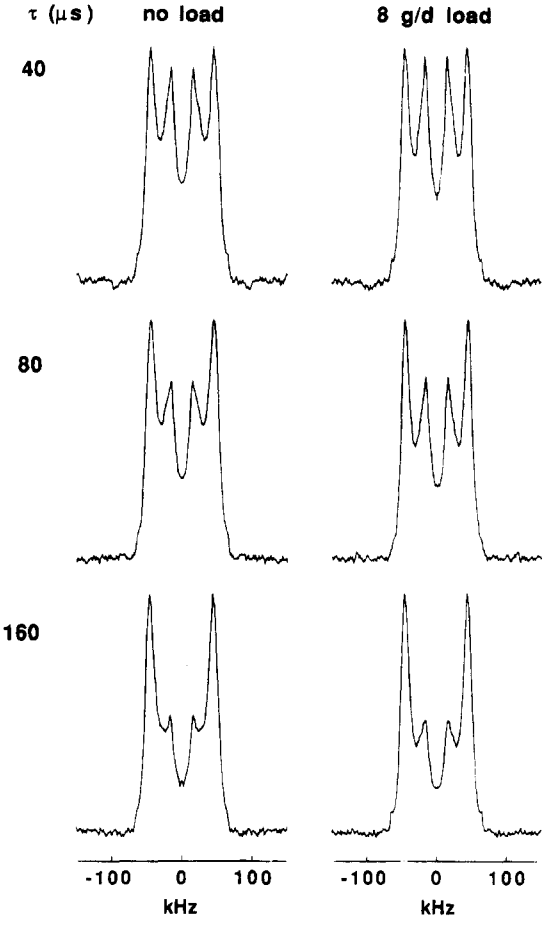

Figure 1. Room temperature ^2H NMR spectra (symmetrized) of heat-treated PPTA-T(d_4) fiber oriented parallel to the external magnetic field as a function of the pulse spacing between quadrupolar echo pulses. Line shapes acquired with no applied tensile stress (left column) are compared to line shapes for the fiber under a tensile stress of the order of 55% of the breaking strength (right column).

ture for the three delay times of 40, 80, and 160 μs between the pulses. No significant tension was applied to the sample (tension of the order of 0.25 g/d was applied to keep the fiber bundle well-aligned and single fibers well-oriented) for the spectra displayed in the left column. The first noticeable difference between these spectra of the highly-oriented fiber and spectra[3] (not shown) of the as-polymerized polymer with an isotropic distribution of C−D bond orientations is a pronounced reduction in the spectral width due to the narrow range of C−D bond orientations possible in the fiber. Furthermore, as for the as-polymerized polymer, the overall line shape is a composite of essentially two spectra: the outer singularities belong to the essentially rigid line shape of the oriented fiber whereas the prominent inner singularities belong to the motionally averaged line shape of rapidly flipping phenylene rings (see below). The inhomogeneously broadened line shape spans a range of 90 kHz and from the frequency position of the outer singularities of the $\tau = 40$ μs spectrum in Figure 1, the maximum angle the C−D bonds form with respect to the external magnetic field can be calculated to be ~73°. The assignment of the prominent inner singularities to the motionally averaged line shape of rapidly flipping phenylene rings is confirmed by the pronounced τ dependence of the line shapes in Figure 1; the intensity of the prominent inner singularities is substantially attenuated, demonstrating that this feature is associated with sites undergoing substantial molecular

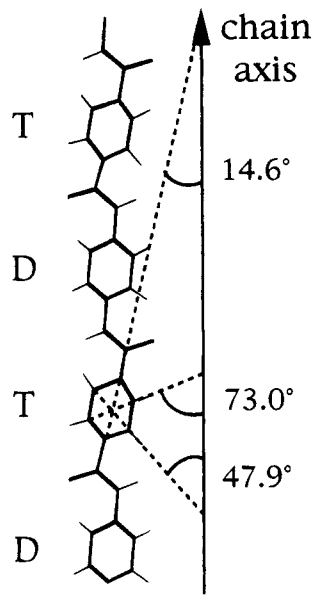

Figure 2. Schematic diagram of a segment of a PPTA molecule illustrating the orientation of the terephthalamide ring 1,4-axis and the C−D bonds with respect to the c-axis as derived from the X-ray structure.

motion. These prominent inner singularities virtually mask two additional singularities associated with the outer singularities; these additional inner singularities are due to the C−D bonds oriented at the minimum possible angle with respect to the magnetic field. In fact, a small shoulder on the outer sides of the prominent inner singularities (due to the C−D bonds undergoing π-flips) is due to C−D bonds which make an angle of ~47° with respect to the magnetic field.

For a *perfectly* oriented crystal with the 1,4-axes of the phenylene rings parallel to the external magnetic field, all C−D bonds would form an angle of 60° relative to the magnetic field and a doublet of narrow lines (with a very small splitting) would be observed in the ^2H NMR spectrum. (The assumption that the 1,4-axes of the phenylene rings are parallel to the external magnetic field also implies that the phenylene ring 1,4-axes are parallel to both the chain and fiber axes—which are assumed to be parallel to the magnetic field.) Figure 2 illustrates the molecular structure of PPTA and the geometrical relationship between the molecular chain axis and the terephthalamide symmetry axis. Inclination of the 1,4-axis of the phenylene ring from the chain axis causes the two sets of *ortho* and *meta* C−D bond pairs to be magnetically distinct; two limiting cases are possible. If the phenylene ring plane is fixed at a certain rotational angle around the 1,4-axis[39] only two C−D bond orientations (one for each *ortho*−*meta* pair) are possible and, consequently, four narrow lines would be observed in the NMR spectrum. If many orientations of the phenylene rings with respect to rotation around the 1,4-axis were possible, then an inhomogeneously broadened line shape with four broadened singularities would be observed. Additionally, inclusion of distributions of C−D bond orientations either through distributions of crystallite and/or fiber-axis orientations would also lead to an inhomogeneous broadening of the line shape as described above. From the width of the experimental NMR line shape alone, the total orientational angle distribution cannot be very large (less than ±10°). Also, once again, the experimental results are not consistent with any type of orientational distribution

where the 1,4-axis of the phenylene ring coincides with the fiber axis.[40,41]

The 73 and 47° extreme values of the orientations of the C−D bonds with respect to the chain axis, derived from the NMR data, are in very good agreement with the C−D bond orientations derived from the X-ray diffraction data.[10] [The X-ray results find an angle of 14.6° between the crystallite *c*-axis and the 1,4-axis of the terephthalamide ring and a ~30° rotation of the ring plane from the plane defined by the *c*-axis and the direction of the hydrogen bonding (amide plane). See Figure 2.] There are a variety of other factors that would need to be taken into account if a more detailed analysis of the NMR data were to be attempted. For instance, this simple model does not take into account either the pleated sheet structure[23] (which leads to a ±5° deviation of the crystallite *c*-axis from the fiber axis perpendicular to the crystallite *b*-axis) or possible distributions of *c*-axes and fiber orientations. Moreover, a distribution of *c*-axis orientations of 13° (full width at half-maximum, FWHM) is known from the X-ray diffraction data.[10] Furthermore, the previously developed description of the heterogeneous structure of as-polymerized polymer[4,6] suggests that the line shape of the oriented sample may more realistically be composed of contributions from a more perfectly ordered (and presumably more perfectly oriented) material (from the interior of the crystallites) and from much less perfectly ordered material (from chains residing mostly at or close to the surface of the crystallites). This level of structural heterogeneity leads to another difficulty in comparing the X-ray diffraction characterization of orientation with that derived from the NMR data: the X-ray results are substantially weighted toward the more highly ordered portions of the polymer, whereas the NMR data reflect all sites with equal weighting (as long as anisotropic T_2 effects caused by molecular motions with rates comparable to the spectral width do not lead to severe distortions in the quadrupolar-echo line shape).

Preliminary NMR line shape simulations which explicitly account for the pleated sheet structure and the *c*-axis distribution, but omit any motional averaging of the line shape, have been carried out. These simulations produce line shapes which differ only slightly from those obtained for the simplified model discussed above; most notably, the position of the outer singularities remains unchanged. The simulations further reveal that any distribution of fiber-axis orientations is unlikely to exceed 12° (FWHM). This value for the distribution of fiber-axis orientations is strongly supported by the experimental 2D ^{2}H NMR spectrum displayed in Figure 3. This spectrum was acquired with a mixing time of 1 s and shows only the contribution of the slowly relaxing component (see below). Both the diagonal and the off-diagonal intensities of the 2D spectrum contain information about the orientational distribution. For a jump-type process,[42] such as a π-flip, the diagonal spectrum is identical to a one-dimensional spectrum. The off-diagonal intensity results from slowly flipping phenylene rings and traces part of the full elliptical pattern obtained for the case of an isotropic distribution. For the geometry of the PPTA fiber the partial elliptical ridges extend further into the 2D plane when the orientational distribution is larger. Since the two elliptical ridges in the experimental spectrum do not overlap, the standard deviation of a Gaussian distribution of *c*-axes and/or fiber axes is no larger than 5° (alternatively, 12° FWHM). These results may also

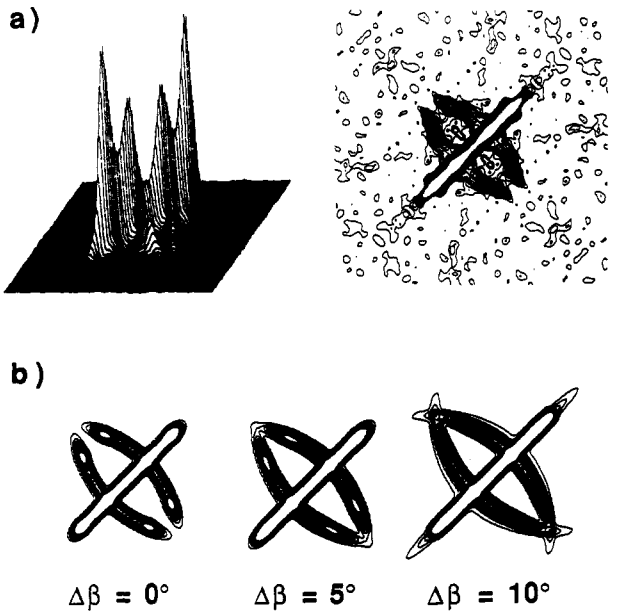

Figure 3. (a) Room temperature 2D ^{2}H NMR spectrum (symmetrized) of heat-treated PPTA-T(d_4) fiber oriented parallel to the external magnetic field; mixing time 1 s. (b) Contour plots of simulated 2D exchange line shapes for three different widths of the distribution of fiber axis angles (β). The values indicate the standard deviation ($\Delta\beta$) of a Gaussian distribution $P(\beta) = \exp(-\sin^2(\beta)/2\sin^2(\Delta\beta))$.

be compared to recent one-dimensional ^{15}N NMR[43] and multidimensional ^{13}C MAS NMR[44] analyses of the orientational distribution of *chopped* commercial PPTA fibers which found full widths at half-heights of Gaussian distributions of 38 and 31°, respectively. Clearly, the orientational distributions derived from these other NMR approaches are severely compromised by the sample preparation method.

To summarize, any attempt to extract a more detailed orientational distribution from the NMR line shapes is complicated by the simultaneous contribution of orientational and motional effects to the line shape. Separation of these two effects is not simple but could, in principle, be achieved by measurement of temperature dependent spectra (to follow the dynamical behavior) or angular dependent spectra (to characterize the orientational distribution). Also, as indicated previously, results for the as-polymerized polymer suggest that the dynamic structure is characterized by a broad distribution of correlation times, which makes it difficult to more precisely quantify the extent of orientational disorder in the fiber. In this regard the pronounced τ-dependence observed in the line shapes of Figure 1 would seem to indicate a significant narrowing of the width of the distribution of correlation times for π-flipping for the oriented fiber as compared to the as-polymerized polymer (where essentially no τ dependence was observed). However, we have also observed that quadrupolar-echo line shapes of fibers oriented orthogonal to the static magnetic field do not exhibit any τ dependence. These observations demonstrate that the orientational and motional effects are strongly coupled. The motional effects upon the line shapes (both π-flipping and librational processes) could be largely eliminated by acquisition of low-temperature NMR data; this is not currently experimentally feasible.

Spin−lattice relaxation of the terephthalamide rings in the fiber is nonexponential and can be decomposed into two components whose relaxation times differ by a factor of 25 or more. The relative amplitudes of the two

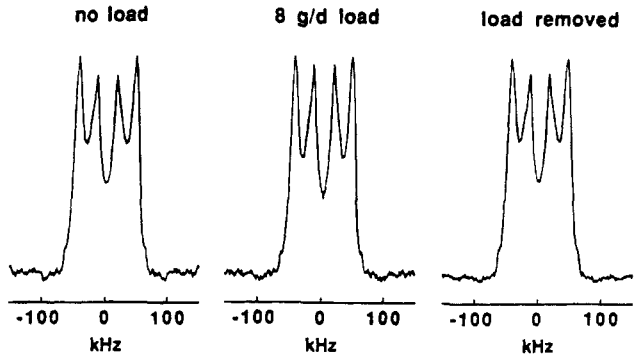

Figure 4. Room temperature ^{2}H NMR spectra (symmetrized) of heat-treated PPTA-T(d_4) fiber oriented parallel to the external magnetic field. Line shapes for $\tau = 40$ μs acquired before (left) and after (right) applying tensile stress are compared to line shapes for the fiber under a tensile stress of the order of 55% of the breaking strength (center).

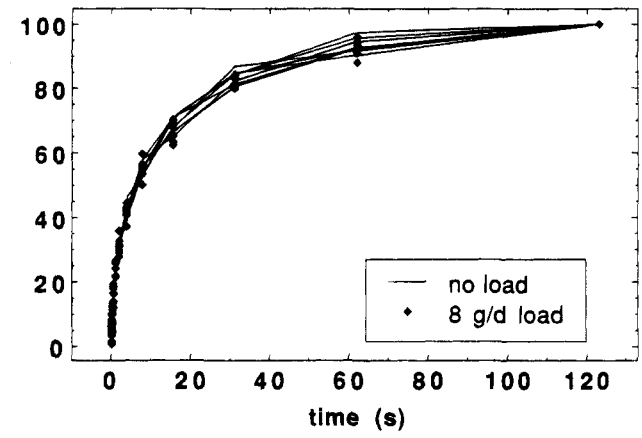

Figure 5. Comparison of ^{2}H NMR spin–lattice magnetization amplitudes as a function of the recovery time in a saturation recovery experiment for PPTA-T(d_4) fiber with and without the application of tensile stress. The five data sets for fibers under load are represented by the symbols. Solid lines connect data points for seven data sets for fibers with no load.

populations are 75% for the contribution with the longer relaxation time and 25% for the component with the shorter relaxation time. Similar amplitudes were found for all three selectively deuterated sites (amide, terephthalamide, or diamine moieties) in the as-polymerized polymer over a temperature range of −184 to +75 °C and were associated with the chains predominantly residing in the interior or at the surface of the crystallites, respectively. Chain segments, or more precisely amide sites at the crystallite surfaces, cannot all hydrogen-bond and thus are able to execute large angle jumps (or possibly large amplitude librations). These mobile amide sites give rise to the spin–lattice relaxation time differentiation of not only the amide sites but also the terephthalamide and diamine ring sites, into two populations of 75% less mobile and 25% more mobile. In the fiber formation process, the mean crystallite size is increased from ~35 Å for the as-polymerized polymer to ~50 Å for the fiber dried at ambient temperature and approximately ~60 Å for the heat-treated fiber. Although the fiber formation process produces crystallites of substantially larger lateral dimensions, the process evidently does not produce a sufficiently large change in the perfection of the amide sites so as to modify their spin–lattice relaxation behavior significantly.

Large Stress. The right hand column of Figure 1 shows quadrupolar-echo line shapes of the fiber when a tensile stress of approximately 8 g/d (1.1 GPa) or 55% of the breaking strength of the fiber bundle is applied. By comparison of the stressed and nonstressed line shapes for $\tau = 40$ μs, it is obvious that tensile stress does not result in a significant change in the orientational distribution of the fiber, since the positions of the broad singularities in the line shapes are virtually unchanged. However, one visible effect is an increase, with stress, of the intensity of the inner singularities associated with fast flipping phenylene rings. In addition, the differences in the τ dependence of the line shapes as a function of stress support the interpretation that the stress-induced changes of the line shape are caused mainly by differences in motional characteristics rather than by orientational aspects. Concomitant with the enhanced mobility of the phenylene rings is an increase in total volume (~0.4% at 0.85% strain), as well as free volume, for a material with a Poisson's ratio of ~0.2–0.3.[45] To demonstrate that the small increase of the intensity of the inner singularities is indeed due to an elastic deformation, Figure 4 compares three $\tau = 40$ μs line shapes, one before load was applied, one with load applied, and one after the load was removed. The line shapes before and after the application of tensile stress are identical and show the same decreased intensity of the inner singularities as compared to the line shape with the application of tensile stress. The complete reversibility of the line shape changes confirms that the mechanical deformation process is *totally elastic*.

Figure 5 compares the ^{2}H NMR spin–lattice magnetization amplitudes as a function of the recovery time in a saturation recovery experiment for a fiber bundle with and without tensile stress. The five data sets obtained for the fiber under tensile stress (symbols) overlap completely with the seven data sets for the fiber without stress (solid lines). For this reason, it can be concluded that the application of tensile stress does not produce a detectable effect upon the restricted, local, very high frequency molecular motions (librations) responsible for spin–lattice relaxation.

Figure 6 illustrates that the partially relaxed ^{2}H NMR spectra have a larger contribution from the motionally averaged line shape than do the fully relaxed spectra (Figure 1). This observation indicates that a component of the spin–lattice relaxation mechanism is attributable to terephthalamide ring-flipping motions in these fibers which are oriented parallel to the magnetic field; this result may be compared to that found for unoriented polymer where the fully relaxed and partially relaxed spectra are very similar.[3] (The conclusion that the terephthalamide ring-flipping motions contribute to spin–lattice relaxation in these oriented fibers is supported by recent 2D ^{2}H NMR exchange experiments for the *p-phenylenediamine moiety in unoriented PPTA polymer* which find that *p*-phenylene ring flipping contributes to the more rapidly relaxing spin–lattice relaxation component as well.[46]) Nevertheless, the continued presence of a substantial contribution from the essentially rigid line shape reflects the dynamic heterogeneity of this more rapidly relaxing spin–lattice relaxation component. No significant differences are observed for the partially relaxed spectra with and without the application of tensile stress to the fiber bundle. This again reflects the insensitivity of the high-frequency component of the dynamic structure to tensile deformation.

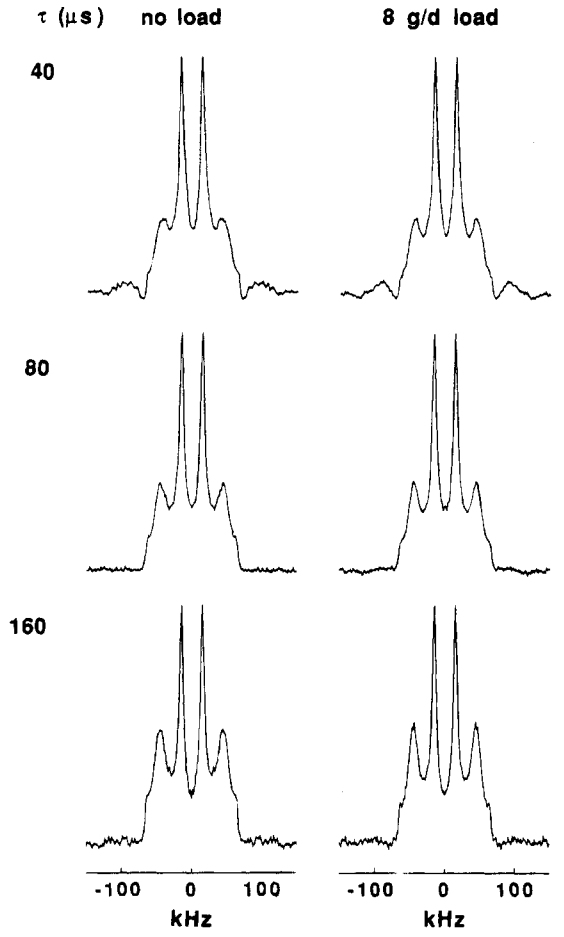

Figure 6. Comparison of room temperature *partially-relaxed* ^2H NMR spectra (symmetrized) of heat-treated PPTA-T(d_4) fiber oriented parallel to the external magnetic field. Line shapes acquired with no applied tensile stress (left column) are compared to line shapes for the fiber under a tensile stress of the order of 55% of the breaking strength (right column).

Conclusions

Solid-state ^2H NMR spectroscopy and X-ray diffraction methods have been used to characterize the dynamic structure of poly(*p*-phenyleneterephthalamide) *continuous* fiber. Spin–lattice relaxation results indicate that the high-frequency component of the dynamic structure is not significantly altered either by the fiber-spinning process utilized here or elsewhere[3] or by the application of tensile stress; hence, this component of the fiber dynamic structure does not differ from that of the as-polymerized polymer. Characterization of the lower frequency components of the dynamic structure by the quadrupolar-echo line shapes associated with the flipping phenylene rings is significantly complicated by the substantial effect that both molecular motion and orientation have on the line shape. The lower frequency dynamics, as reflected by the ring-flipping motion, must be quite heterogeneous to be consistent with the experimental observations.

Quadrupolar-echo line shapes reflect the high degree of order in the fiber. Determination of a detailed orientational distribution from the NMR line shapes is complicated by the simultaneous contribution of orientational and motional effects to the line shape. Nevertheless, the orientational distribution of the C–D bonds of the terephthalamide rings derived from the 2D ^2H NMR spectrum is in very good agreement with the orientational distributions calculated from X-ray data obtained in previous work.[10] The NMR line shapes indicate that the orientational distribution does not change substantially with the application of tension. The X-ray data indicate that the full width at half-height of a Lorentz-IV distribution of crystallite orientations is 13° for a commercial fiber, as compared to our finding of 12° for the full width at half-height of a Gaussian distribution for our laboratory-produced fiber. Furthermore, our use of a *continuous* fiber bundle has been shown to be a much preferred approach as compared to those methods utilizing *chopped* fibers,[43,44] when using solid-state NMR methods to determine orientational distributions.

The application of a macroscopic tensile stress of 8 g/d (equivalent to 55% of the breaking strength of the fiber bundle) alters the NMR line shape, reflecting the coupling between the macroscopic stress and the microscopic dynamic structure through enhanced phenylene ring dynamics. The larger fraction of rapidly flipping terephthalamide rings with the application of stress is attributed to an increase in bulk volume and hence free volume.

Acknowledgment. We are indebted to P. S. O'Connor, Jr. for skilled technical assistance with regard to the preparation and postspinning treatment of the deuterated fiber and C. R. Walther for acquisition of the NMR data.

References and Notes

(1) Cain, E. J.; Gardner, K. H.; Gabara, V.; Allen, S. R.; English, A. D. *Polym. Prepr. (Am. Chem. Soc., Div. Polym. Chem.)* **1990**, *31*, 518.
(2) Cain, E. J.; Gardner, K. H.; Gabara, V.; Allen, S. R.; English, A. D. *Macromolecules* **1991**, *24*, 3721.
(3) Schadt, R. J.; Cain, E. J.; Gardner, K. H.; Gabara, V.; Allen, S. R.; English, A. D. *Macromolecules* **1993**, *26*, 6503.
(4) Schadt, R. J.; Gardner, K. H.; Gabara, V.; Allen, S. R.; Chase, D. B.; English, A. D. *Macromolecules* **1993**, *26*, 6509.
(5) Schadt, R. J.; Cain, E. J.; Gardner, K. H.; Gabara, V.; Allen, S. R.; English, A. D. *Polym. Prepr. (Am, Chem. Soc., Div. Polym. Chem.)* **1991**, *32*, 253.
(6) Jackson, C. L.; Schadt, R. J.; Gardner, K. H.; Chase, D. B.; Allen, S. R.; Gabara, V.; English, A. D. *Polymer* **1994**, *35*, 1123.
(7) English, A. D.; Gardner, K. H.; Schadt, R. J.; Cain, E. J.; Gabara, V.; Allen, S. R. *Polym. Prepr. (Am. Chem. Soc., Div. Polym. Chem.)* **1992**, *33*, 82.
(8) Panar, M.; Avakian, P.; Blume, R. C.; Gardner, K. H.; Gierke, T. D.; Yang, H. H. *J. Polym. Sci., Polym. Phys. Ed.* **1983**, *21*, 1955.
(9) Northolt, M. G.; Hout, R. v. d. *Polymer* **1985**, *26*, 310.
(10) Northolt, M. G. *Polymer* **1980**, *21*, 1199.
(11) Allen, S. R.; Roche, E. J. *Polymer* **1989**, *30*, 996.
(12) Young, R. J.; Lu, D.; Day, R. J.; Knoff, W. F.; Davis, H. A. *J. Mater. Sci.* **1992**, *27*, 5431.
(13) Li, Y.; Wu, C.; Chu, B. *J. Polym. Sci.; Part B: Polym. Phys.* **1991**, *29*, 1309.
(14) Chu, B.; Wu, C.; Li, Y.; Harbison, G. S.; Roche, E. J.; Allen, S. R.; McNulty, T. F.; Phillips, J. C. *J. Polym. Sci., Part C: Polym. Lett.* **1990**, *28*, 227.
(15) Young, R. J.; Lu, D.; Day, R. *J. Polym. Int.* **1991**, *24*, 71.
(16) Prasad, K.; Grubb, D. T. *J. Appl. Polym. Sci.* **1990**, *41*, 2189.
(17) Chang, C.; Hsu, S. L. *Macromolecules* **1990**, *23*, 1484.
(18) Edwards, H. G. M.; Hakiki, S. *Br. Polym. J.* **1989**, *21*, 505.
(19) Zwaag, S. v. d.; Northolt, M. G.; Young, R. J.; Robinson, I. M.; Galiotis, C.; Batchelder, D. N. *Polym. Commun.* **1987**, *28*, 276.
(20) Galiotis, C.; Robinson, I. M.; Young, R. J.; Smith, B. J. E.; Batchelder, D. N. *Polym. Commun.* **1985**, *26*, 354.
(21) Penn, L.; Milanovich, F. *Polymer* **1979**, *20*, 31.
(22) Northolt, M. G.; Van Aartsen, J. J. *J. Polym. Sci., Polym. Symp.* **1977**, *58*, 283.
(23) Dobb, M. G.; Johnson, D. J.; Saville, B. P. *J. Polym. Sci., Polym. Phys. Ed.* **1977**, *15*, 2201.
(24) Allen, S. R.; Roche, E. J. *Polymer* **1989**, *30*, 996.
(25) Roche, E. J.; Wolfe, M. S.; Suna, A.; Avakian, P. *J. Macromol. Sci., Phys.* **1985**, *B24*, 141.

(26) Roche, E. J.; Allen, S. R.; Fincher, C. R.; Paulson, C. *Mol. Cryst. Liq. Cryst.* **1987**, *153*, 547.
(27) Yang, H. H.; Chouinard, M. P.; Lingg, W. J. *J. Appl. Polym. Sci.* **1987**, *34*, 1399.
(28) Egorov, E. A.; Zhizhenkov, V. V. *J. Polym. Sci., Polym. Phys. Ed.* **1982**, *20*, 1089.
(29) Deloche, B.; Samulski, E. T. *Macromolecules* **1981**, *14*, 575.
(30) Dickinson, L. C.; Shi, J.-F.; Chien, J. C. W. *Macromolecules* **1992**, *25*, 1224.
(31) Hansen, M. T.; Boeffel, C.; Spiess, H. W. *Colloid Polym. Sci.* **1993**, *271*, 446.
(32) Hansen, M. T.; Bluemich, B.; Boeffel, C.; Spiess, H. W.; Morbitzer, L.; Zembrod, A. *Macromolecules* **1992**, *25*, 5542.
(33) Hansen, M. T.; Kulik, A. S.; Prins, K. O.; Spiess, H. W. *Polym. Commun.* **1992**, *33*, 2231.
(34) Tanner, D.; Fitzgerald, J. A.; Phillips, B. R. *Adv. Mater.* **1989**, *51*, 151.
(35) Yang, H. H. *Aromatic High Strength Fibers*; SPE Monographs; Wiley-Interscience: New York, 1989.
(36) Schadt, R. J.; English, A. D. *J. Magn. Reson., Ser. A* **1994**, *108*, 244.
(37) Schaefer, D. J.; Leisen, J.; Spiess, H. W. Manuscript in preparation.
(38) Schmidt, C.; Blümich, B.; Spiess, H. W. *J. Magn. Reson.* **1988**, *79*, 269.
(39) Simpson, J. H.; Rice, D. M.; Karasz, F. E. *Macromolecules* **1992**, *25*, 2099.
(40) Hong, J.; Harbison, G. S. *Polym. Prepr. (Am. Chem. Soc., Div. Polym. Chem.)* **1990**, *31*, 115.
(41) Hempel, G.; Schneider, H. *Pure Appl. Chem.* **1982**, *54*, 635.
(42) Leisen, J.; Boeffel, C.; Dong, R. Y.; Spiess, H. W. *Liq. Cryst.* **1993**, *14*, 215.
(43) Yeo, J.-H.; Demura, M.; Asakura, T.; Fujito, T.; Imanari, M.; Nicholson, L. K.; Cross. T. A. *Solid State NMR* **1994**, *3*, 209.
(44) Wilhelm, M.; Féaux de Lacroix, S.; Titman, J. J.; Schmidt-Rohr, K.; Spiess, H. W. *Acta Polym.* **1993**, *44*, 279.
(45) Nakamae, K.; Nishino, T.; Airu, X. *Polymer* **1992**, *33*, 4898.
(46) Schaefer, D. J.; English, A. D. *Polymer*, in press.

MA941231R